ICSO 2016

International Conference on Space Optics

Biarritz, France

18–21 October 2016

Photopolymer materials for volume phase holographic optical elements

A. Zanutta

E. Orselli

T. Fäcke

A. Bianco

PHOTOPOLYMER MATERIALS FOR VOLUME PHASE HOLOGRAPHIC OPTICAL ELEMENTS

A. Zanutta[1], E. Orselli[2], T. Fäcke[2] and A. Bianco[1].
[1]INAF – Osservatorio Astronomico di Brera, via Bianchi 46, 23807, Merate (LC), Italy.
[2]Covestro AG, Kaiser-Wilhelm-Allee 60,51373 Leverkusen, Germany
alessio.zanutta@brera.inaf.it, enrico.orselli@covestro.com, thomas.faecke@covestro.com,
andrea.bianco@brera.inaf.it

INTRODUCTION

Volume Phase Holographic Gratings (VPHGs) cover a relevant position as dispersing elements in spectrographic instrumentations with low and medium resolution. This is due to their unique properties especially in terms of diffraction efficiency. These devices have to provide dispersion, resolving power, bandwidth and diffraction efficiency according to the target scientific and technological cases. Custom gratings can be designed and manufactured to match the requirements and maximize the performances.

The design and manufacturing of high efficiency and reliable VPHGs require photosensitive materials where it is possible to finely control the refractive index modulation, which is the key property that determines the efficiency together with the film thickness. Photopolymers are a promising class of holographic materials since they can address precisely the refractive index modulation; moreover, they are self-developing, meaning that no chemical process is required after the light exposure.

We studied a specific family of photopolymers, Bayfol® HX by Covestro AG, which show: i) a large tuning capabilities; ii) a good transparency over the visible and NIR spectral range and iii) a large refractive index modulation. The structure of these materials consists in a double layer film that can be easily laminated onto the substrate, with many advantages like compactness, flexibility and environmental stability.

Based on such good materials, we designed and manufactured dispersing elements for astronomical instrumentations: ALFOSC (The Andalucia Faint Object Spectrograph and Camera) mounted on the Nordic Optical Telescope (2.56 meters, La Palma, Spain) and AFOSC (Asiago Faint Object Spectrograph and Camera) mounted onto Asiago's telescope in Italy.

Such devices provided to the instrument the advantage to match exactly the astronomical requirements for the scientific cases, with a system throughput gain that, in some cases, surpassed the 80%.

I. VPHG'S DESIGN GUIDELINES AND THEORY

In the design of a VPHG, after having satisfied the dispersion and the resolution requirements which fix parameters like the line density (Λ) of the grating, the incidence and diffraction angles (α and β respectively), the design process can move to the optimization of the diffraction efficiency (both peak efficiency and bandwidth).

The main parameters to be considered in this case are: i) the refractive index modulation Δn, ii) the film thickness d and iii) the slanting angle, i.e. the angle between the normal of the grating surface and the normal of the refractive index modulation plane.

Considering a sinusoidal refractive index modulation and working in the Bragg regime (the light is sent only in one diffraction order other than the zero), the well-known Kogelnik model can be used to understand the behavior of the grating that has to be designed [1].

According to this model, the diffraction efficiency of a transmission VPHG for unpolarized light at the Bragg angle (incidence angle equal to the diffraction angle) obeys to the classical Kogelnik equation and for small angles, large diffraction efficiency is achieved when the product Δn × d is equal to half of the wavelength. This is usually the right starting point where to begin the optimization of the design.

As already stressed, not only the peak efficiency is important, but also the efficiency at the edges of the spectral range and according to the Kogelnik model, the spectral bandwidth of the diffraction efficiency curve is proportional to [2]:

$$\frac{\Delta\lambda}{\lambda} \propto \cot\frac{\alpha}{\Lambda\,d}. \tag{1}$$

In this equation, it is evident that the bandwidth is inversely proportional to Λ and the thickness of the grating. Therefore, the optimization of the efficiency curve (changing Δn and *d*) provides large differences in the grating response. If a grating works in the Bragg regime, the largest peak efficiency and bandwidth is obtained for very

thin films and large Δn. Of course, the upper value of Δn is determined by the performances of the holographic material.

Out this condition, the VPHG works in the Raman-Nath regime [3] and it diffracts the light with a non-negligible efficiency in more than one diffraction order. Consequently, for low dispersion gratings, it is better to increase the film thickness and reduce the Δn in order to have a large peak efficiency and bandwidth. The smaller the Λ parameter, the smaller the required Δn and larger d.

Nevertheless, a VPHG working at higher wavelengths requires larger values of Δn and/or d to achieve the same efficiency performances, both if it works in the Raman-Nath and Bragg regimes. Fig. 1 summarizes these guidelines.
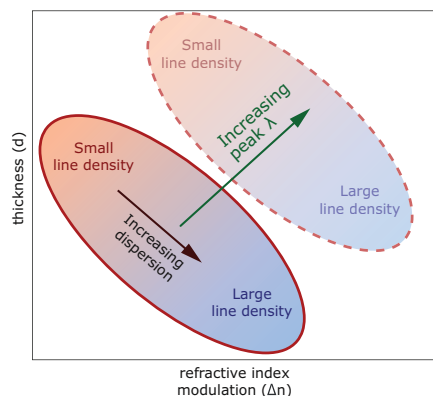

Fig. 1. Scheme reporting the general rules for designing high efficient and wideband VPHGs in the $d - \varDelta n$ space.

From the point of view of holographic materials, the main issue for low Λ VPHGs is the manufacturing of thick holographic films preserving the optical quality and providing a uniform thickness, but at the same time addressing the $\varDelta n$ to a well-defined value. On the opposite, for high Λ VPHGs, the main issue is to push the $\varDelta n$ as high as possible and to make very thin film with constant thickness. Of course, for every condition, a holographic material suitable for the manufacturing of high performances VPHGs should show a tunable modulation of the refractive index together with a wide range of thicknesses to reach the desired performances.

II. PHOTOPOLYMERIC MATERIAL CHARACTERIZATION

The newly [4-6] developed photopolymer film technology (Bayfol® HX film) evolved from efforts in holographic data storage (HDS) [4-7] where any form of post processing is unacceptable. These new instant developing recording media open up new opportunities to create vHOEs for new diffractive optics and have proven to be able to record predictable and reproducible optical properties. This was demonstrated recently also for transmission holograms and directional diffusors [5-9].

Bayfol® HX represents a technology platform of customized holographic recording films. Depending on the application requirements, the substrate can be varied toward characteristics like thickness, (low) birefringence and optical flatness. The photopolymer layers can be designed towards e.g. (high or low) index modulation, transparency, wavelength sensitivity (monochromatic or RGB) and required thickness to match the gratings wavelength and/or angular selectivity.

The Bayfol® HX films consist of a three-layer stack of substrate, light-sensitive photopolymer and protective cover film. The protective cover film must be removed so the photopolymer film can be index matched by simply laminating it on glass plates.

Among this family, we initially characterized a research level sample showing a nominal thickness of 16 μm, RGB sensitive and a PA (polyamide) substrate of 60 μm;

A. Spectral characterization

In order to understand the usability spectral range of Bayfol® HX material, we recorded the transmission spectrum before and after the light exposure to incoherent white light with a fluence of ~ 50 J/cm² (Fig. 2). As can be seen in the figure the behavior in the NIR spectral region is dominated by the polymer substrate. Indeed, the material is transparent up to 2.2 μm, where the infrared overtones of the polyamide start to absorb strongly. It seems that no evident absorptions come from the photopolymer system. In the UV region, the photopolymer shows a steep transition opaque to transparent at 312 nm. Moreover, in the unexposed film, we clearly identify

the absorption peaks of the sensitizers that make the material panchromatic. After the bleaching step, some weak residual absorption bands are present in the visible. In general, higher residual absorption occurs increasing the film thickness and this is especially true approaching the UV cut-off. Therefore, a particular attention must be paid to VPHGs working in this region, where the absorption could reduce the final VPHG's diffraction efficiency.
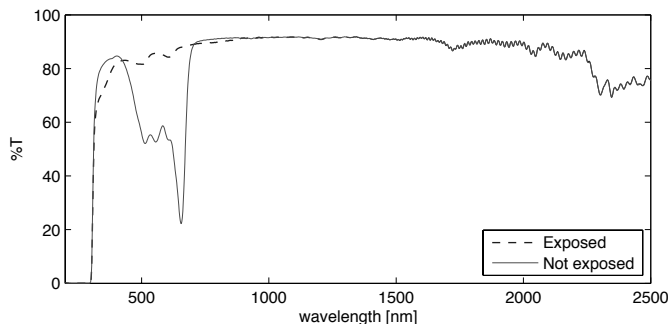

Fig. 2. UV-vis-NIR spectra of the Bayfol® TP16 photopolymeric material before (solid line) and after photo-bleaching (dashed line).

B. Tunability: Δn as function of power density and beam ratio intensity

As previously anticipated, the most wanted property of a holographic material for volume diffraction grating is the ability to tune the refractive index modulation, in order to assess the spectral requirements that have been defined in the design phase.

The Bayfol® HX photopolymeric material generates the index difference through a reaction-diffusion mechanism, which involves a competing process between the migration of the monomers inside the film and the polymerization of the material itself [10]. The photopolymerization occurs in the exposed regions of the pattern (constructive interference), while due to a concentration gradient, the monomers migrate from the dark to the exposed regions being polymerized themselves.

The photopolymerization of this system depends upon the writing power density [11]. Therefore, increasing the writing power, the monomer conversion occurs with a higher velocity competing with the diffusion mechanism. For this reason, the maximum achievable index modulation starts to drop.

This behavior finds confirmation in the data presented in Figure 3, which reports the values of *Δn* as function of the writing power density ranging from 0.143 to 21.5 mW/cm^2 for samples with increasing line density (600, 1000, 1400 l/mm). The total illumination dose was kept constant at 42 mJ/cm^2, therefore the exposure times for each sample changed accordingly.
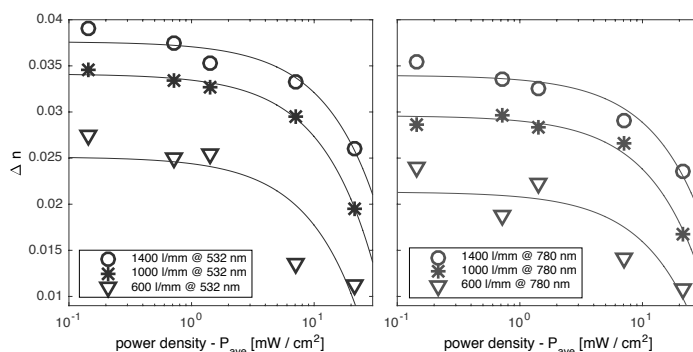

Fig. 3. *Δn* as function of the mean value of the intensity of the two writing arms. The total dose was kept constant at 42 mJ/cm^2 (referred to double beam writing process).

Another peculiar effect that is visible in figure, is the dependence of *Δn* on the line density: the curves of samples with higher line densities are shifted at larger *Δn* values. This effect is again easily understandable if we think at the reaction-diffusion mechanism of the photopolymer. An Increased Λ value means a shorter path to travel for the monomer, thus a facilitated process of *Δn* formation. This is true in the range of line density here considered, for much higher Λ, a *Δn* cut-off could occur because of the nonlocal effects. It is important to notice that Bayfol® HX photopolymers showed a much smaller nonlocal response parameter, which turns into a larger resolution in comparison with standard AA/PVA photopolymers [12].

We also notice a dependence of the *Δn* with the wavelength. This could be ascribed to the dispersion of the refractive index with the light frequency; by increasing the frequency, the refractive index increases (normal dispersion). Such increment changes in the exposed and unexposed regions because of the different polarizability. In particular, we could expect a more pronounced rise of refractive index for the exposed regions, with a consequent growth of *Δn* for shorter wavelengths, as experimentally verified. Moreover, the amount of change is compatible with the chemical composition of the photopolymer system.

Another possible strategy for the *Δn* tuning is related to the intensity ratio of the two holographic writing beams. It is well known that in order to obtain the largest contrast in the interference pattern, the intensity of the two laser beams must be as equal as possible. This is for sure the best achievable condition for maximizing the refractive index modulation while, if lower *Δn* values have to be achieved, unbalanced writing intensities can be used.

We have also evaluated this behavior performing writings at different ratios, while maintaining constant the total irradiation dose at 42.8 mJ/cm^2. The outcome was a strong dependence of the *Δn* with the intensity ratio occurs, confirming that the best condition for the recoding of transmission VPHGs is the balanced (50:50) beam ratio, but lower values can be addressed precisely when different ratios are set. This strategy is especially useful when very low *Δn* values are required and high values of laser power cannot be provided to constrain the *Δn* with the balanced beams.

From these results, it is evident how with this material we can achieve precise *Δn* values in accordance with the design goals, in a range strictly related to the lines per millimeter of the target VPHG. For example, if we need a diffraction grating with 1400 l/mm and we can deal with powers from 0.143 to 21.5 mW/cm^2, the achievable *Δn* can be from 0.026 to 0.039.

III. PRACTICAL CASE: OPTIMIZATION OF DISPERSIVE ELEMENTS FOR AN ASTRONOMICAL SPECTROGRAPH

Based on the good properties of Bayfol® HX, we designed and manufactured dispersing elements for astronomical instrumentation. The main purpose was to upgrade the existing dispersing devices based on ruled gratings, taking advantage of the increase in efficiency with an overall effect that is comparable to the increase of the telescope size. The target instrumentation was the FOSC spectrograph (Faint Object Spectrograph and Camera) [12], in particular, ALFOSC (The Andalucia Faint Object Spectrograph and Camera) mounted on the Nordic Optical Telescope (2.56 meters, La Palma, Spain) and AFOSC (Asiago Faint Object Spectrograph and Camera) mounted onto Asiago's telescope in Italy. The dispersing elements in the FOSC are GRISMs (Grating with prISMs) with a clear aperture of 38 mm. After the design phase, which included critical steps like the calculation of the grating's key parameters (incidence angles α and pitch Λ) to match the dispersion and resolution criteria and the simulation of the efficiency response, the manufacturing of the VPHG and the integration of the GRISMs have been performed. In total six GRISMs were produced, three for ALFOSC and three for AFOSC [13,14].

A. ALFOSC devices

The three elements for ALFOSC are characterized by a resolving power of approximately 1000 and they cover the 350-1000 nm spectral range. In Table 1, the specifications of the devices that were named #18, #19 and #20 according to the telescope's internal numeration are reported.

Table 1. NOT's delivered GRISMs main specifications summary: (1) Working central wavelength of the grating; (2) pixel dispersion of the grating; (3) Wavelength range; (4) Resolution, R = λ/Δλ; (5) pitch of the grating; (6) final refractive index modulation of the grating; (7) prism apex angle (the prisms were in BK7).

Device name	Central λ [nm] (1)	Dispersion [Å/px] (2)	Δλ [nm] (3)	Rϕ (4)	l/mm (5)	Δn (6)	Prism apex angle (°)
#18	430	0.918	337 – 523	1129	1086	0.019	24.80
#19	562	1.212	443 – 687	1110	823	0.023	20.75
#20	788	2.079	576 – 1000	896	484	0.022	24.80

In the case of the devices #19 and #20, a coloured filter has been embedded to cut the second order spectrum, which had a non-negligible efficiency. For the device #18, devoid of order sorting filter, the coupling fluid OCF-452 has been used instead of cedar oil in order to shift the UV cut-off at shorter wavelengths, granting a high transmittance (60%/mm) even at 330 nm. To completion of the description, we report in Table 2 the diffraction efficiencies of the three transmission GRISMs that we have manufactured for ALFOSC. The measurements were completed in laboratory before the commitment at the telescope and they were performed at different wavelengths. As has been reported, each device possesses a different spectral range, therefore is not possible to present the efficiency data all at the same wavelength. It is evident from the table how each device, for wavelengths inside its own spectral range, possess very high overall efficiencies, that in most cases surpass the 80%.

Table 2. ALFOSC GRISMs transmission efficiencies at different wavelengths. The values correspond to raw measurements, without reflection losses corrections or materials absorption corrections.

Device name	Wavelength [nm] - Efficiency [%]
GRISM #18	457 – 83
	514 – 57
GRISM #19	633 – 73
	532 – 85
GRISM #20	633 – 80
	780 – 88

After the integration into the telescope, the GRISMs are compared with similar gratings, in terms of dispersion, spectral range and resolution, which were already available in the spectrograph. In Figure 4, for example, can be seen the spectra of photometric-standard star SP0305+261 taken with one of our device in comparison with the already mounted one. It is evident that the throughput of the VPHGs surpasses the ruled dispersive element in the spectral region of interest. In some cases, (e.g. GRISM #18 vs. #16, Figure 1) a gain of 85% is reached, meaning that the exposition time to have the same S/N (signal to noise ratio) is nearly halved.
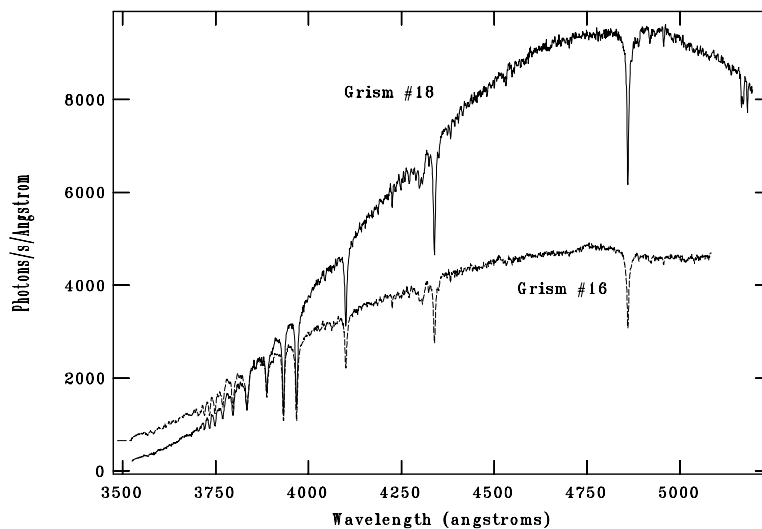

Fig. 4. Comparison of photometric-standard stars' spectra SP0305+261. Total system throughput of the NOT telescope with Grism #16 and Grism #18. Slitwidth used in the observations is 10.0 arcsec.

The GRISM #20 has been successfully used to observe the source SDSS J004054.65-0915268 which was a candidate for being a high redshift (z = 5.00) bright BLLAC object3 (i = 18.2). With the integration of this new GRISM with extended range, we had the opportunity to confirm the featureless nature of this object from 9000 to 10000 Å, targeting the C IV strong emission line in its near-IR spectrum. In that case this source could be the farthest known BLLACs at that redshift. In any case if its BLLAC nature will not be confirmed it would be anyway an interesting source for spectroscopic studies (weak emission lines QSOs5) [13].

B. AFOSC devices

In the past decade, the AFOSC instrument already took advantage of the Volume Phase Holographic Grating technology thanks to six newly designed DCG based dispersive elements [15]. Those innovative GRISMs well matched the most important spectral features observable with Asiago's spectrograph with an improved resolution up to R = 5000. Following the procedure of the NOT's devices described in the previous section, we designed and produced three new photopolymer based VPHG GRISMs for the AFOSC spectrograph. The astronomical specifications of these devices are reported in Table 3.

Table 3. Asiago's delivered GRISMs main specifications summary: (1) Working central wavelength of the grating; (2) pixel dispersion of the grating; (3) Wavelength range; (4) Resolution, $R = \lambda/\Delta\lambda$; (5) pitch of the grating; (6) final refractive index modulation of the grating; (7) prism apex angle. *) single non-right triangle.

Device name	Central λ [nm] (1)	Dispersion [Å/px] (2)	$\Delta\lambda$ [nm] (3)	R (4)	l/mm (5)	Δn (6)	Prism apex angle (°)
VPHG6	800	0.90	620 – 980	720	285	0.011	12.7
VPHG7	525	2.95	350 – 800	458	280	0.007	A=4.4 + B=12.7 *
VPHG8	700	1.40	550 – 800	1380	600	0.017	22.8

Two of the elements show a low dispersion (ca. 280 l/mm with R=500–700), while the third (VPHG8) has 600 l/mm and a resolution of 1300. As we discussed before, VPHGs at very low dispersion (line density) require low Δn and thick films. Achieving precise low Δn is not straightforward with the risk to send too much light into unwanted diffraction orders. In Table 4 we report the diffraction efficiencies of the three GRISM that we have manufactured for AFOSC. The measurements were completed in laboratory before the commitment at the telescope and they were performed at different wavelengths.

Table 4. AFOSC GRISMs transmission efficiencies at different wavelengths. The values correspond to raw measurements, without reflection losses corrections or materials absorption corrections.

Device name	Wavelength [nm] - Efficiency [%]
VPHG6	670 – 78 808 – 89
VPHG7	405 – 58 532 – 69
VPHG8	670 – 90 808 – 77

The VPHG6 was designed for observations of supernovae, while the VPHG8 was aimed for the inspection of the Hα region with a very high efficiency. Details of these VPHGs were already been published by the authors [16].

The most interesting device among these GRISMs is the VPHG7, which shows a novel architecture based on slanted fringes VPHG and only one BK7 prism (Figure 7), with advantages such as less production costs and number of optical interfaces, reducing the reflection losses and the risk of ghosts [17]. This novel design was chosen because the target astronomical application required the highest possible near-UV efficiency and the minimisation of the number of layers and interfaces allowed us to produce a dispersive element with a good efficiency down to 3500 Å.
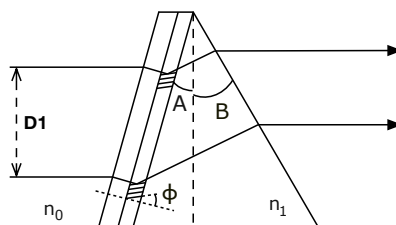

Fig. 5. Scheme of the VPHG7 single GRISM with slanted fringes, ϕ is the slanting angle, A and B the prism apex angles, D1 the illuminating beam diameter.

Figure 6 reports the comparison between the throughput of the single prism GRISM VPHG7 with the corresponding ruled GRISM commonly used to observe the bluest part of the objects' spectra. It is apparent the shift in the efficiency curve at shorter wavelengths. There is not a large increase in the peak efficiency and this is due to the low line density of the grating (280 l/mm). Indeed, for low line density gratings, also the ruled gratings showed a good efficiency. On the other hand, by a suitable choice of low UV absorption materials like substrates and coupling fluids a huge increase in the efficiency is achieved up to 4300 Å.
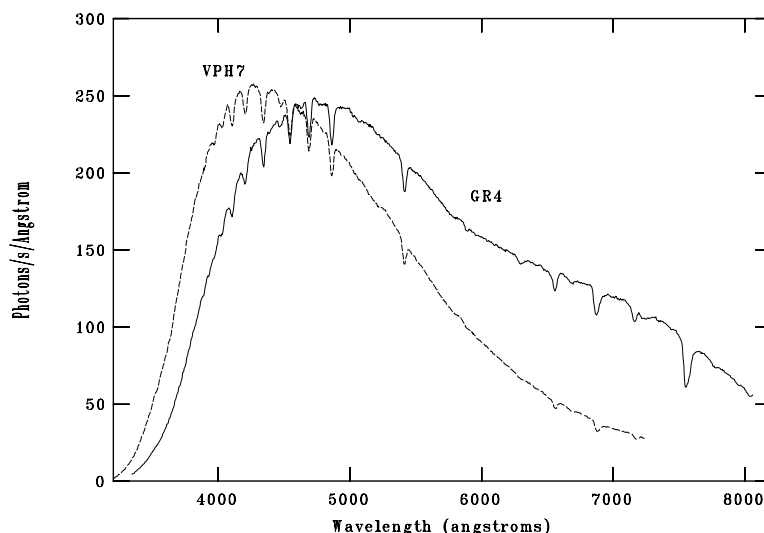

Fig. 6. Comparison of photometric-standard stars' spectra. Total system throughput of the Asiago's telescope with GRISM VPHG7 and grating GR4. Slitwidth used in the observations is 4.22 arcsec.

IV. CONCLUSIONS

In this paper, we reported on the study of Bayfol® HX photopolymers, focusing on the characterization of this material for the specific production of astronomical diffraction holographic elements. We pointed out some hints required in the design phase in order to address specifically the astronomical requirements for each scientific case. Such materials are interesting in comparison to the common DCGs mainly thanks to the self-developing behaviour and the ability to easily obtain custom index modulation values.

Six GRISMs were developed for two FOSC instruments, namely ALFOSC (@NOT) and AFOSC (@Asiago Telescope) working in the 3500 – 10000 Å spectral range with a resolution ranging from 500 to 1000. The combination of d and Δn allowed to obtain the target efficiency curve both in terms of peak efficiency and bandwidth. The full GRISMs preserve the large efficiency of the VPHG meaning that the coupling losses (between prisms and substrates) are very small as the absorption and scattering components.

Thanks to the on-sky tests of dispersing elements belonging to the class of VPHGs that were manufactured using Bayfol® HX photopolymers we demonstrated that Bayfol® HX materials are suitable materials for the production of VPHGs with low and medium dispersion not only at the laboratory level, but at the astronomical instrumentation level.

ACKNOWLEDGEMENTS

REFERENCES

[1]   H. Kogelnik, "Coupled-wave theory for thick hologram gratings," Bell System Technical Journal 48, 2909-2947 (1969).

[2]   S. C. Barden, J. A. Arns, W. S. Colburn, and J. B. Williams, "Volume-phase holographic gratings and the efficiency of three simple volume-phase holographic gratings," Publications of the Astronomical Society of the Pacific 112(772), 809-820 (2000).

[3]   M. G. Moharam, and L. Young, "Criterion for Bragg and Raman-Nath diffraction regimes," Applied Optics 17(11), 1757-1759 (1978).

[4]   F. Bruder, and T. Fäcke, "Materials in optical data storage," International Journal of Materials Research 101(2), 199-215 (2010).

[5]   H. Berneth, F. K. Bruder, T. Fäcke, R. Hagen, D. Hönel, D. Jurbergs, T. Rölle, and M.-S. Weiser, "Holographic recording aspects of high-resolution Bayfol® HX photopolymer," Proc. SPIE 7957, 79570H (2011).

[6]   H. Berneth, F.-K. Bruder, T. Fäcke, R. Hagen, D. Hönel, T. Rölle, G. n. Walze, and M.-S. Weiser, "Holographic recordings with high beam ratios on improved Bayfol® HX photopolymer," Proc. SPIE 8776, 877603 (2013).

[7]   L. Dhar, K. Curtis, and T. Fäcke, "Holographic data storage: Coming of age," Nat Photon 2(7), 403-405 (2008).

[8]   F.-K. Bruder, F. Deuber, T. Fäcke, R. Hagen, D. Hoenel, D. Jurbergs, M. Kogure, T. Roelle, and M.-S. Weiser, "Full-Color Self-processing Holographic Photopolymers with High Sensitivity in Red - The First Class of Instant Holographic Photopolymers," Journal of Photopolymer Science and Technology 22(2), 257-260 (2009).

[9]   F.-K. Bruder, F. Deuber, T. Fäcke, R. Hagen, D. Hoenel, D. Jurbergs, T. Roelle, and M.-S. Weiser, "Reaction-diffusion model applied to high resolution Bayfol® HX photopolymer," Proc. SPIE 7619, 76190I (2010).

[10]   R. Jallapuram, I. Naydenova, H. J. Byrne, S. Martin, R. Howard, and V. Toal, "Raman spectroscopy for the characterization of the polymerization rate in an acrylamide-based photopolymer," Applied Optics 47(2), 206-212 (2008).

[11]   M. R. Gleeson, J. T. Sheridan, F.-K. Bruder, T. Rölle, H. Berneth, M.-S. Weiser, and T. Fäcke, "Comparison of a new self developing photopolymer with AA/PVA based photopolymer utilizing the NPDD model," Optics Express 19(27), 26325-26342 (2011).

[12]   AFOSC user manual. http://archive.oapd.inaf.it/asiago/5000/5100/ man01_2.ps.gz. Accessed: 2014-09-29.

[13]   Landoni, M., Zanutta, A., Bianco, A., Tavecchio, F., Bonnoli, G., and Ghisellini, G., "Optical spectroscopy of SDSS J004054. 65-0915268: three possible scenarios for the classification. A z\ sim 5 BL Lacertae, blue FSRQ or a weak emission line quasar". The Astronomical Journal, 151, 2, pp 35, (2016).

[14]   Zanutta, A., Bianco, A., Landoni, M., Tomasella, L., Benetti, S., and Giro, E., "New GRISMs for AFOSC based on volume phase holographic gratings in photopolymers" Proc. SPIE 91474E-91474E, (2014).

[15]   Bianco, A., Molinari, E., Conconi, P., Crimi, G., Giro, E., Pernechele, C. and Zerbi, F.M. "VPHG in the cold". In Astronomical Telescopes and Instrumentation, pages 22–30. International Society for Optics and Photonics, (2003).

[16]   Zanutta, A., Landoni, M., Bianco, A., Tomasella, L., Benetti, S., and Giro, E., "A New Photopolymer-based VPHG for Astronomy: The Case of SN 2013fj". Publications of the Astronomical Society of the Pacific, 126(937), 264, (2014).

[17]   Burgh, E., Bershady, M., Westfall, K., & Nordsieck, K., "Recombination Ghosts in Littrow Configuration: Implications for Spectrographs Using Volume Phase Holographic Gratings". Publications of the Astronomical Society of the Pacific, 119(859), 1069-1082, (2007).